NASA CR-72285
NBS REPORT 9293

INTERIM REPORT

CAVITATION INCEPTION IN LIQUID NITROGEN AND LIQUID HYDROGEN FLOWING IN A VENTURI

by D. K. Edmonds, J. Hord, and D. R. Millhiser

Prepared under Contract No. C-35560-A
for
NATIONAL AERONAUTICS AND SPACE ADMINISTRATION

Prepared by
U.S. Department of Commerce
NATIONAL BUREAU OF STANDARDS
Boulder, Laboratories
Boulder, Colorado

NOTICE

This report was prepared as an account of Government sponsored work. Neither the United States, nor the National Aeronautics and Space Administration (NASA), nor any person acting on behalf of NASA:

A.) Makes any warranty or representation, expressed or implied, with respect to the accuracy, completeness, or usefulness of the information contained in this report, or that the use of any information, apparatus, method, or process disclosed in this report may not infringe privately owned rights; or

B.) Assumes any liabilities with respect to the use of, or for damages resulting from the use of any information, apparatus, method or process disclosed in this report.

As used above, "person acting on behalf of NASA" includes any employee or contractor of NASA, or employee of such contractor, to the extent that such employee or contractor of NASA, or employee of such contractor prepares, disseminates, or provides access to, any information pursuant to his employment or contract with NASA, or his employment with such contractor.

Requests for copies of this report should be referred to

National Aeronautics and Space Administration
Office of Scientific and Technical Information
Attention: AFSS-A
Washington, D. C. 20546

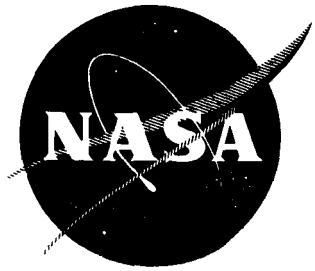

NASA CR- 72285
NBS REPORT 9293

INTERIM REPORT

CAVITATION INCEPTION IN LIQUID NITROGEN AND LIQUID HYDROGEN FLOWING IN A VENTURI

by D. K. Edmonds, J. Hord, and D. R. Millhiser

prepared for
NATIONAL AERONAUTICS AND SPACE ADMINISTRATION
CONTRACT No. C-35560-A
August, 1967

Technical Management
NASA Lewis Research Center
Cleveland, Ohio
Liquid Rocket Technology Branch
Werner R. Britsch

NBS - U. S. Department of Commerce, Boulder, Colorado

FOREWORD

This report was prepared by the National Bureau of Standards, Institute for Materials Research, United States Department of Commerce under Contract C-35560-A. The contract was administered by the Lewis Research Center of the National Aeronautics and Space Administration, Cleveland, Ohio. The work summarized in this report was performed during the period 15 July 1964 to 15 July 1967. The NASA project manager for the Contract was Mr. Werner R. Britsch. Mess'rs. R.S. Ruggeri, T. F. Gelder, and R. D. Moore of the Fluid Systems Components Division at NASA Lewis Research Center---under the direction of M. J. Hartmann---served as research consultants and technical advisers during the course of this program.

TABLE OF CONTENTS

ILLUSTRATIONS

ILLUSTRATIONS (continued)

TABLES

Interim Report

CAVITATION INCEPTION IN LIQUID NITROGEN AND LIQUID HYDROGEN FLOWING IN A VENTURI

by

D. K. Edmonds, J. Hord, and D. R. Millhiser

ABSTRACT

Cavitation characteristics of liquid hydrogen and liquid nitrogen in a transparent plastic venturi have been determined. The experimental data are presented in tabular and graphical form. Conventional cavitation-parameter and head-velocity curves are given over the range of experimental temperatures (36.5 to 41°R for hydrogen and 140 to 170°R for nitrogen) and inlet velocities (70 to 185 ft/sec for hydrogen and 20 to 70 ft/sec for nitrogen). Minimum local wall pressure was calculated to be less than bulk stream vapor pressure by as much as 323 feet of hydrogen head and 63 feet of nitrogen head.

1. Introduction

Cavitation is usually defined as the formation, caused by a reduction in pressure, of a vapor phase within a flowing liquid or at the interface between a liquid and a solid. Since the formation and collapse of vapor cavities alters flow patterns, cavitation may reduce the efficiency of pumping machinery[1], and reduce the precision of flow measuring devices. Collapse of these vapor cavities can also cause serious erosion damage[2] to fluid handling equipment.

NASA has undertaken a program[1] to determine various cavitation characteristics of different fluids in an effort to develop design criteria to aid in the prediction of cavitation in pumps. The experimental study described herein was conducted in support of this program. Liquid hydrogen and liquid nitrogen were chosen as test fluids for this study for the following reasons: (1) the ultimate goal of this program is to acquire sufficient knowledge to permit intelligent design of pumps for near-boiling liquids and (2) predictive analyses[1] indicated that the physical properties of hydrogen and nitrogen make them particularly desirable test fluids.

The objective of this study was to determine the flow conditions required to induce cavitation, in liquid hydrogen and liquid nitrogen, on the walls of a transparent plastic venturi. The shape of the venturi was chosen to duplicate the test section used by NASA[3-6]. Tests were conducted with test section inlet velocities of 70 to 185 ft/sec in hydrogen and 20 to 70 ft/sec in nitrogen. Inlet temperatures were varied from 36.5 to 41°R with hydrogen and from 140 to 170°R with nitrogen in order to determine the effects of temperature upon cavitation inception. The data reported here are intended to supplement that given in several NASA technical notes[3-6] for a geometrically similar, but 1.414 times as large, test section. Comparison of NASA and NBS inception data for liquid nitrogen at about 140°R indicates no scale effects. Both incipient and

desinent cavitation data were acquired with no noticeable hysteresis; i.e., the flow conditions corresponding to vapor inception are identical whether the data point is approached from non-cavitating or fully-developed cavitating flow. In this report, incipience refers to the appearance of visible vapor cavities, whether they are due to incipient or desinent cavitation.

2. Apparatus

The facility used for this study consisted of a blow-down system with the test section located between the supply and receiver dewars; see figure 2.1. Dewars and piping were vacuum shielded to minimize heat transfer to the test fluid. Flow control was attained by regulating the supply and receiver dewar pressures. Pressure and volume capacities of the supply and receiver vessels are indicated on figure 2.1. The receiver dewar pressure control valving limited the venturi inlet velocity, V_o, to about 185 ft/sec in hydrogen, while the supply dewar pressure rating limited the inlet velocity to about 70 ft/sec in nitrogen.

Valves located on each side of the test section permit flow stoppage in the event of venturi failure while testing with liquid hydrogen. A plenum chamber was installed upstream of the test section to assure uniform non-cavitating flow at the test section inlet. The supply dewar was equipped with a 5 Kw heater which was used to heat the test fluid.

2.1 Test Section

A photograph of the test section as viewed through one of the windows in the vacuum jacket is shown in figure 2.2. The transparent plastic venturi was flanged into the apparatus using high compression elastomeric "O" rings. Test section details are given in figures 2.3 and 2.4. Referring to figure 2.3, static pressure tap No. 1 was the only instrument port drilled and used in the liquid hydrogen inception tests. Some liquid nitrogen data were acquired with all of the pressure and temperature sensing

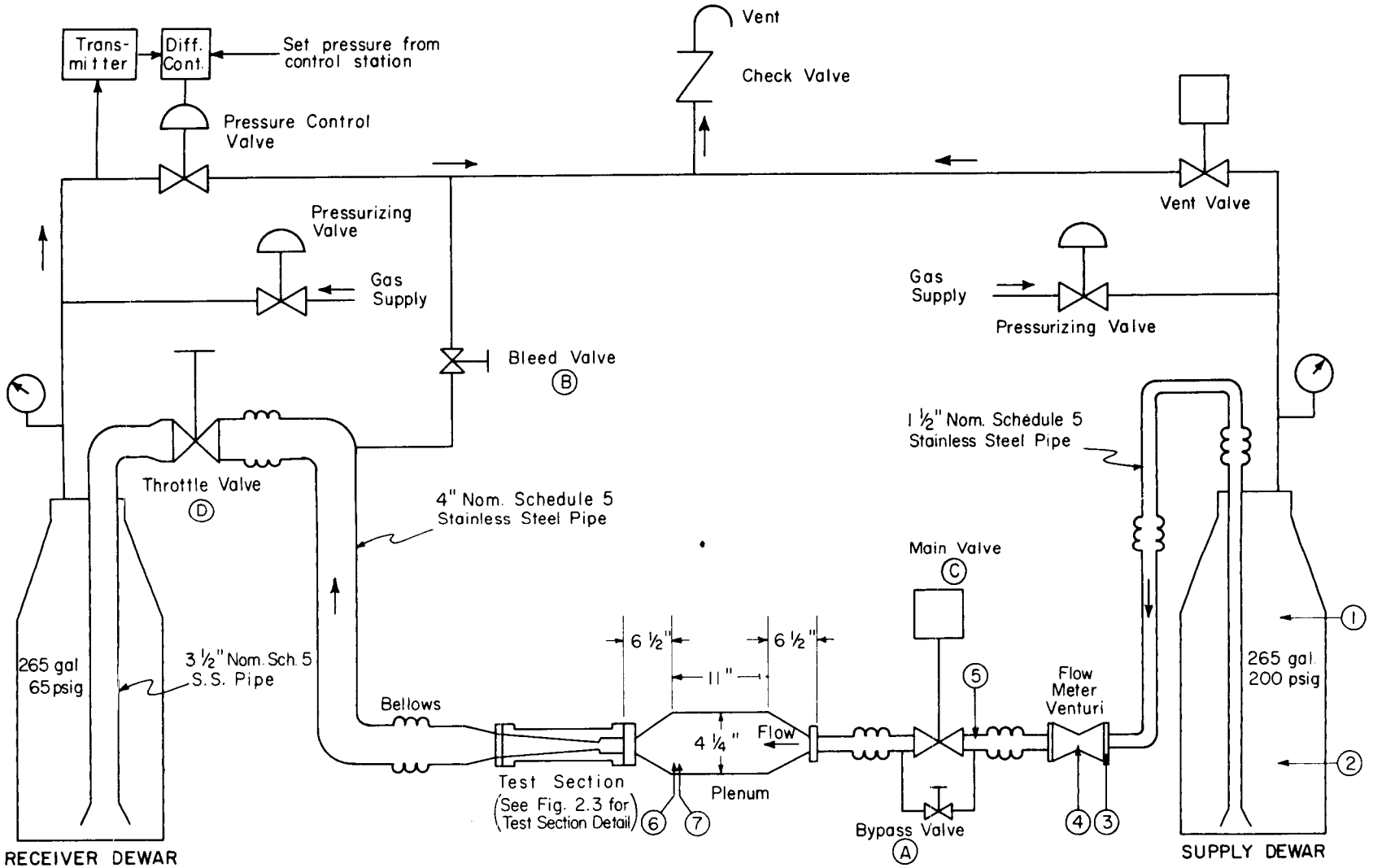

Figure 2.1 Schematic of Cavitation Flow Apparatus.

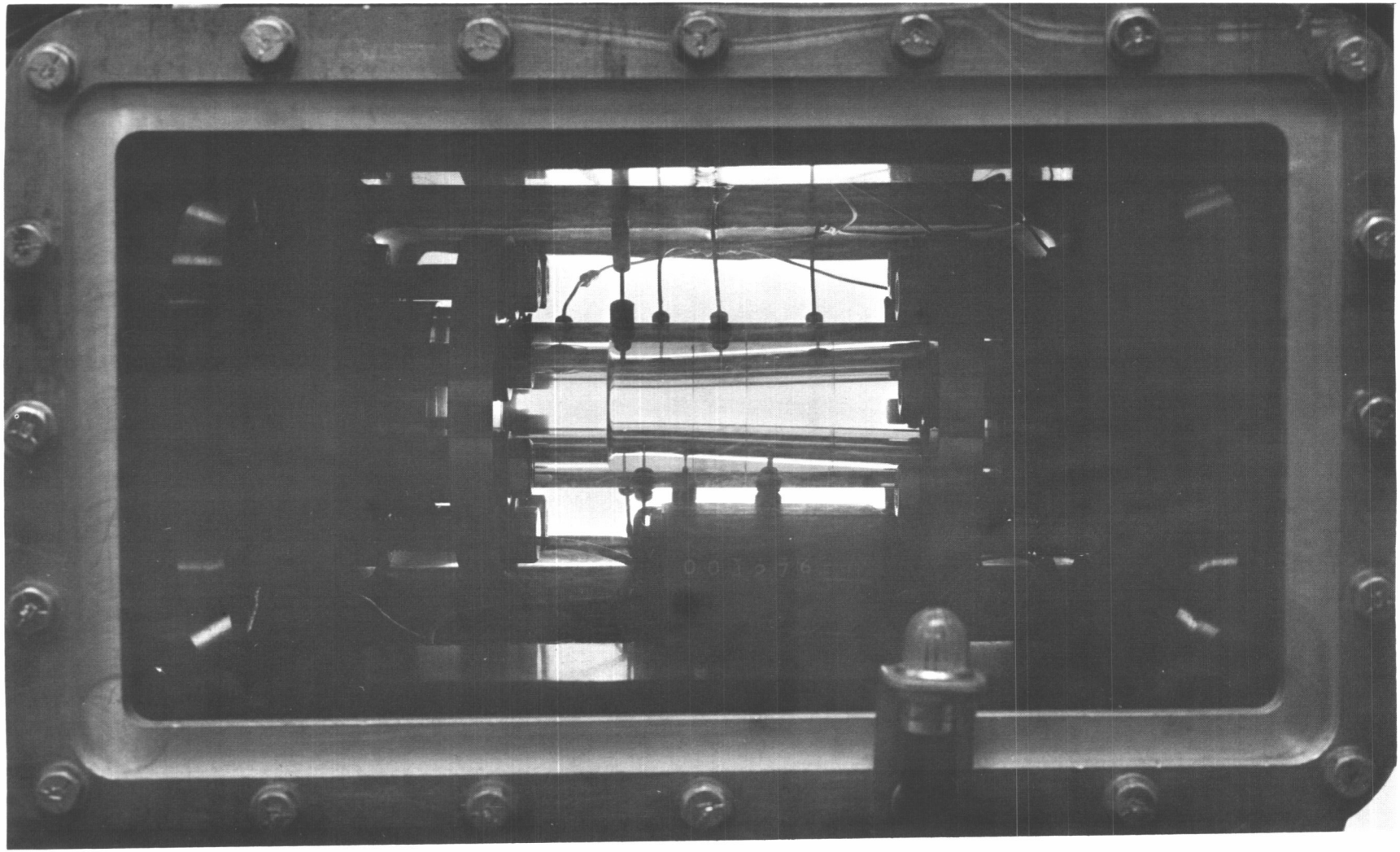

Figure 2.2 Photograph of Plastic Venturi Test Section Installed in System. Note Counter -- Used to Correlate Flow Data with Film Event.

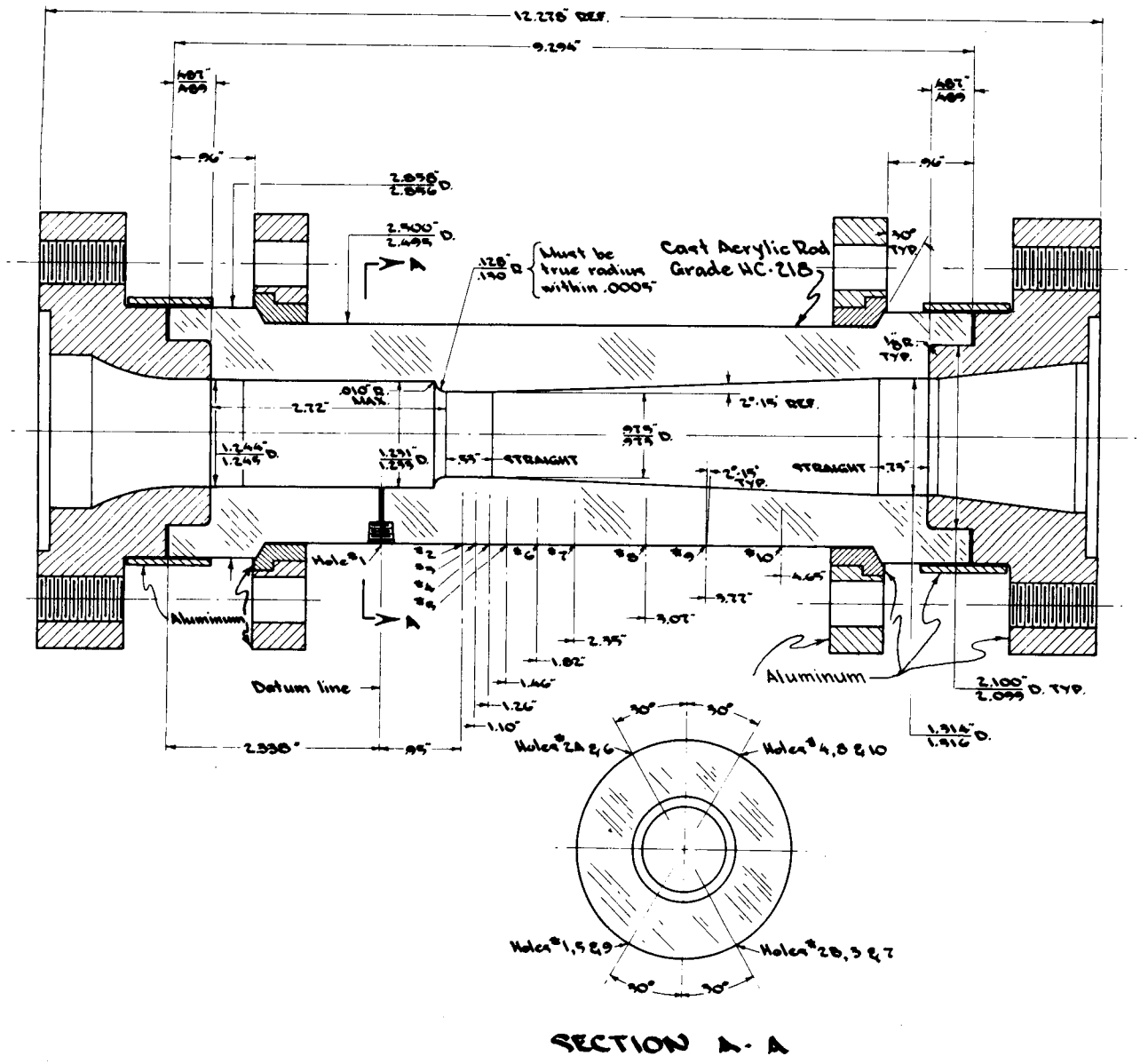

Figure 2.3 Sketch of Plastic Venturi Section Showing Dimensions and Location of Pressure and Temperature Instrumentation.

69875

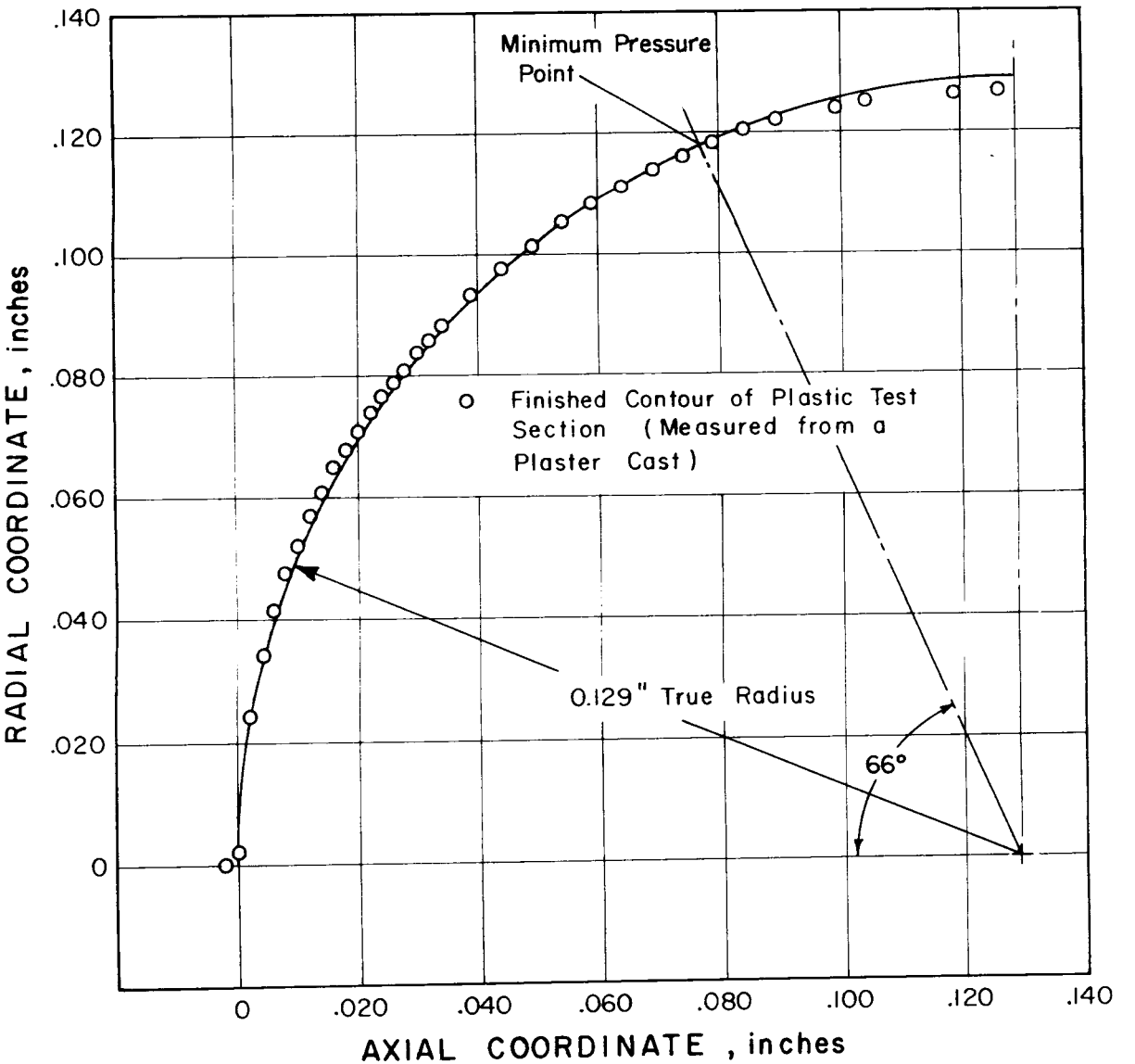

Figure 2.4 Quarter-Round Contour of Convergent Region of Plastic Test Section.

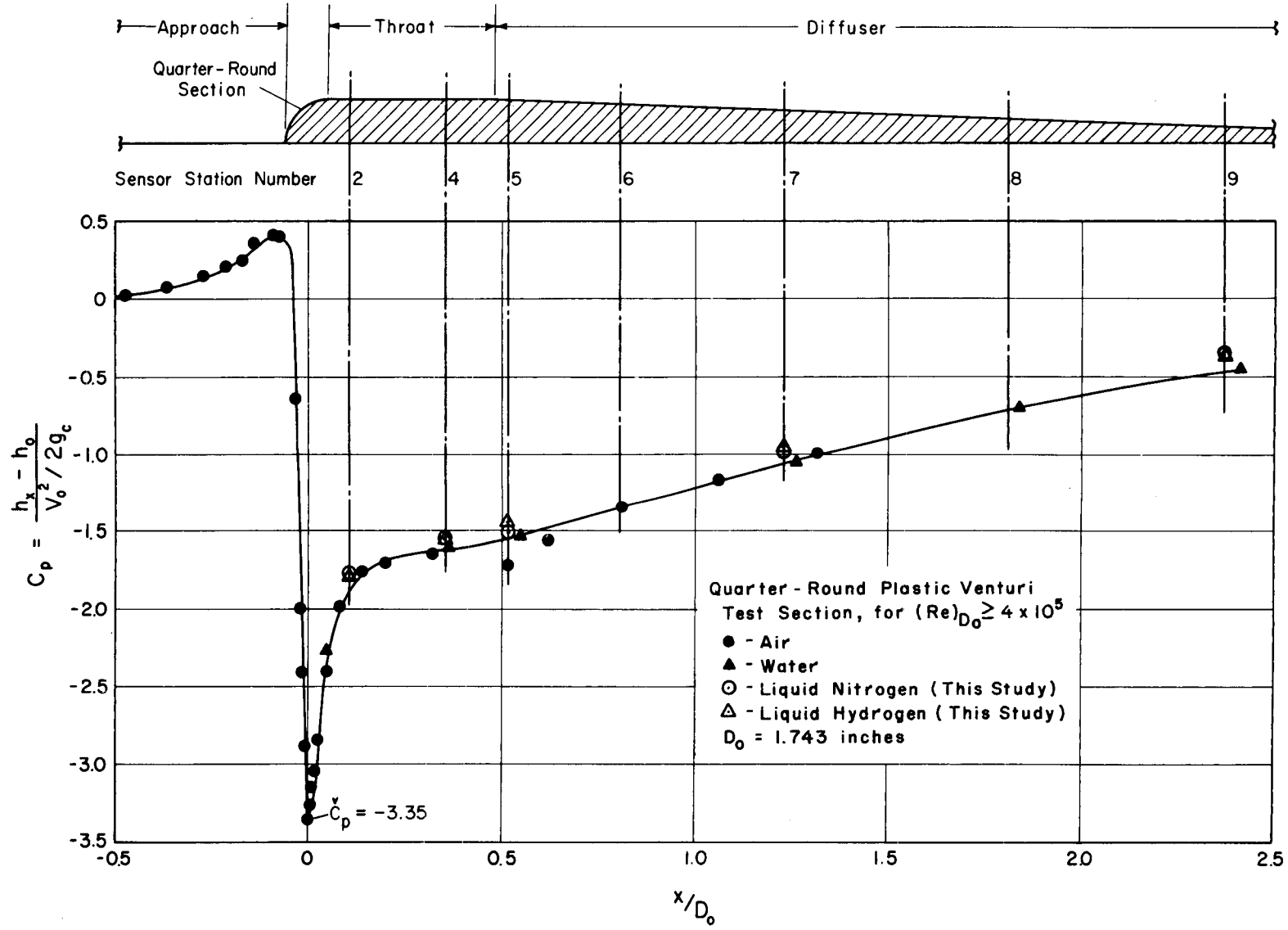

Figure 2.5 Pressure Distribution Through Test Section for Non-Cavitating Flow.

E-70178

ports instrumented, figure 2.2. Since incipient cavitation involves very small cavities at or near the minimum pressure point---see figures 2.4 and 2.5---the presence or absence of the additional sensing ports has no effect on the data reported. The design and as-built venturi contours are shown on figure 2.4. The test section dimensions were checked by using the plastic venturi as a mold for a dental plaster plug. The plug was then removed and measured. Pressure distribution for non-cavitating flow across the quarter-round contour[3,7] is shown in figure 2.5. This pressure profile has been confirmed using several test fluids[3-5] and data from this study, and applies when $(Re)_{D_o} \geq 4 \times 10^5$.

2.2 Instrumentation

Location of the essential instrumentation is shown on figures 2.1 and 2.3.

Liquid level in the supply dewar was sensed with a ten-point carbon resistor rake. Test fluid temperature in the supply dewar was determined by two platinum resistance thermometers, see figure 2.1. Fluid temperatures at the flowmeter and test section inlet were also measured with platinum resistance thermometers. These platinum thermometers were calibrated to provide temperature readings accurate within ±0.04°R. The thermometers were powered with a current source which did not vary more than 0.01 percent. Voltage drop across the thermometers was recorded on a 5 digit electronic voltmeter data acquisition system. The overall accuracy of the temperature measurement is estimated to be within ±0.09°R.

System gage and differential pressure measurements were obtained with pressure transducers mounted in a temperature stabilized box near the test section. Differential pressure measurements were used where possible to provide maximum resolution. The pressure transducers were calibrated via laboratory test gages at frequent intervals during the test

series. Repeatability of the transducers was better than ±0.25 percent and their output was recorded on a continuous trace oscillograph with approximately one percent resolution. The overall accuracy of the pressure measurement, including calibration and read-out errors is estimated to be within ±2.0 percent. Bourdon gages were used to monitor the various tests.

Volumetric and mass flow rates were determined via a Herschel venturi flowmeter designed to ASME Standards[8]. The internal contour of this meter was verified in the same manner as the test venturi. An error analysis of this flow device and associated pressure and temperature measurements indicates an accuracy in mass flow of about one percent.

An electronic pulsing circuit provided a common time base for correlating data between oscillograph, digital voltmeter, and movie film. The data were reduced by first viewing film of the test event. A solenoid-actuated counter, installed adjacent to the test section was energized by the electronic pulser and appears on the film, figure 2.2. Thus, the data are reduced at the desired instant of time by simply matching the number of voltage pulses which have elapsed.

An acoustic cavitation detection device was developed and successfully used to determine cavitation inception. This device was found to be more sensitive than the human eye, i.e., cavitation inception could be detected with the acoustic transducer before it was visible to the unaided eye. Visible incipience is frequently used as the criterion for cavitation inception and is normally reported in the literature since the sensitivity [9-11] of various acoustic detectors can vary appreciably. Although the data presented here are based upon visible incipience, full description of the acoustic transducer is given for reference in Appendix A of this paper.

2.3 Visual and Photographic Aids

Use of a plastic test section, liquid hydrogen, and relatively high pressures precluded direct visual observation; therefore, closed-circuit television was used to observe the tests.

Movies of cavitation tests were taken at approximately 20 frames per second on 16 mm film. The variable speed camera was equipped with a 75 mm lens and synchronized with a high intensity stroboscope, providing a 3 μ-sec exposure. The stroboscope was situated directly opposite the camera lens and illuminated the test section through a plastic diffuser mask; this technique provided a shadow-graph or back-lighting effect and excellent contrast between vapor and liquid phases in the test section.

3. Test Procedure

The following procedure refers to figure 2.1. The supply dewar was filled with test liquid and then some of the liquid was extracted through valves A and B to cool the test section and piping. Approximately two hours were required to cool the plastic test section without breakage. Cooldown was monitored via a platinum resistance thermometer in the plenum chamber. Upon completion of cooldown, the contents of the supply dewar were transferred through the test section into the receiver dewar, and then back into the supply dewar again. This operation cooled the entire flow system in preparation for a test. Next, the liquid in the supply dewar was heated to the desired temperature. Because the test section and connecting piping were kept full of liquid at low pressure during preparatory and calibration periods between tests, the plastic venturi was generally colder than the test liquid. Supply and receiver dewars were then pressurized to appropriate levels and flow started by opening valve C. In the case of non-cavitating flow, inception was induced by lowering the receiver dewar

pressure and thus increasing the flow velocity until vapor appeared. To obtain desinent cavitation from fully developed cavitating flow, the receiver dewar pressure was increased until the vapor cavity was barely visible. Receiver dewar pressure was remotely controlled by means of a pneumatic transmitter, differential controller, and vent valve arrangement, figure 2.1. It was necessary to increase test section back-pressure by means of throttle valve D for some of the liquid nitrogen tests. Flow was terminated by closing valve C. The supply dewar was then vented and the test liquid transferred back into the supply dewar for another test. As previously mentioned, the entire test event was recorded on movie film which was subsequently used to determine incipient and desinent cavitation conditions.

4. Data Analysis and Discussion

All of the useable experimental inception data are given in tables 4.1 and 4.2. These same data points were mathematically temperature-compensated and presented in table 4.3. Derivation of these compensated data is described in Appendix B of this paper.

The conventional cavitation parameter, K_{iv}, for liquid hydrogen is shown on figure 4.1. Little temperature dependency is evident in this plot of experimental data and this prompted the presentation of calculated data given on figures 4.2 and 4.3. The calculated data used in the preparation of figures 4.2 and 4.3 are derived as explained in Appendix B and are presented in table 4.4. The liquid nitrogen data were handled in a similar manner and plotted on figures 4.4 and 4.5 from the calculated data of table 4.5. Photographs of cavitation inception are shown for both test fluids on figures 4.6 and 4.7.

Table 4.1 Cavitation Inception Data for Liquid Hydrogen

Run #	T_o (°R)	V_o (ft/sec)	$\dot{m}$ (lb_m/sec)	h_o (ft, abs)	P_o (psia)	h_v (ft, abs)	P_v (psia)	K_{iv}	$\overset{v}{h}$ (ft, abs)
R026A	36.47	73.6	2.623	614.6	18.87	478.9	14.70	1.61	333.8
R026B	36.77	72.4	2.572	606.1	18.56	505.0	15.45	1.24	334.6
R031A	36.63	132.1	4.713	1244.9	38.26	492.6	15.09	2.78	339.9
031C	36.59	133.1	4.750	1228.0	37.76	488.0	14.95	2.69	309.3
R032	37.22	167.1	5.945	1756.2	53.81	548.1	16.70	2.79	308.1
R034	36.50	106.2	3.788	962.0	29.56	481.8	14.78	2.74	377.1
035	37.19	169.7	6.040	1755.0	53.81	538.0	16.40	2.72	261.5
R036	37.67	108.2	3.819	1062.0	32.36	585.0	17.75	2.62	454.9
R037	37.55	134.7	4.769	1362.6	41.56	573.7	17.43	2.80	421.7
R038	38.21	170.5	6.010	1822.0	56.36	638.4	19.27	2.62	309.8
R039	36.99	184.9	6.599	1973.5	60.66	524.0	16.00	2.73	200.5
040	37.40	185.6	6.600	2042.5	62.56	560.8	17.06	2.77	256.1
R040	37.55	183.3	6.511	2051.5	62.76	574.1	17.44	2.83	309.1
043A	37.03	180.6	6.440	1906.0	58.56	524.0	16.00	2.73	214.5
043B	36.97	180.0	6.420	1902.0	58.46	521.0	15.90	2.74	221.7
049	36.63	91.0	3.241	802.7	24.62	492.3	15.08	2.41	373.2
051	36.85	91.2	3.241	825.3	25.27	511.2	15.63	2.43	394.2
052	38.00	92.6	3.257	915.1	27.72	616.5	18.65	2.24	470.4
054	40.64	125.0	4.288	1577.3	46.62	931.6	27.45	2.66	767.6
056	40.79	154.3	5.298	1989.3	58.82	951.5	28.00	2.81	754.1
057	40.91	174.1	5.975	2303.9	68.12	969.0	28.47	2.84	732.9
058	40.88	124.3	4.254	1604.8	47.32	964.3	28.35	2.67	804.2
059	40.70	120.2	4.120	1507.4	44.52	939.1	27.66	2.54	758.8

Table 4.2 Cavitation Inception Data for Liquid Nitrogen

Run #	T_o (°R)	V_o (ft/sec)	$\dot{m}$ (lb_m/sec)	h_o (ft, abs)	P_o (psia)	h_v (ft, abs)	P_v (psia)	K_{iv}	$\overset{v}{h}$ (ft, abs)
005B	138.08	19.27	7.86	49.7	17.45	38.71	13.6	1.9	30.44
021RR	169.34	61.68	22.51	374.1	117.6	232.4	72.9	2.4	176.80
022RR	168.2	64.54	23.68	379.7	120.0	219.5	69.2	2.48	163.68
024RR	152.91	66.44	25.83	276.5	92.6	98.4	32.9	2.60	47.58
095	140.3	33.70	13.65	86.3	30.1	45.34	15.81	2.32	27.40
099	161.1	33.90	12.77	184.6	59.9	154.1	50.0	1.71	125.00
100	150.75	43.21	16.91	154.3	52.0	87.05	29.32	2.32	57.47
105	161.0	67.1	25.33	334.6	108.8	153.2	49.7	2.59	101.11
106A	166.45	65.45	24.18	368.6	117.3	201.8	64.08	2.51	164.45
106B	166.4	66.67	24.64	367.9	117.1	201.2	63.9	2.42	137.39
107	150.88	70.62	27.66	298.8	100.8	87.68	29.52	2.73	40.16
108	140.87	65.39	26.47	229.7	80.1	47.08	16.39	2.75	7.95
109	140.76	72.05	29.19	268.3	93.6	46.75	16.28	2.75	-.92
110	140.72	43.64	17.66	111.6	38.9	46.54	16.21	2.20	12.84
111A	161.15	49.92	18.81	240.1	77.9	154.5	50.15	2.21	110.86
111B	161.08	50.76	19.13	240.6	78.1	154.1	50.0	2.16	106.98
112	140.63	47.90	19.39	128.8	44.9	46.27	16.12	2.32	9.81

Table 4.3 Experimental Data Points Which Have Been Temperature Compensated by Means of Equation [10-3] for Hydrogen and Equation [10-4] for Nitrogen

Run #	Nominal Temp (°R)	h_o (ft, abs)	V_o (ft/sec)	Run #	Nominal Temp (°R)	h_o (ft, abs)	V_o (ft/sec)	Run #	Nominal Temp (°R)	h_o (ft, abs)	V_o (ft/sec)
				HYDROGEN							
R026A	36.5	616.3	73.6	R037	37.5	1357.9	134.7	051	36.5	801.9	91.2
R026B	36.5	590.3	72.4	R038	37.5	1742.5	170.5	052	37.5	875.1	92.6
R031A	36.5	1234.2	132.1	R039	36.5	1921.5	184.9	054	41.0	1623.8	125.0
031C	36.5	1220.6	133.1	040	37.5	2054	185.6	056	41.0	2019.2	154.3
R032	37.5	1785.9	167.1	R040	37.5	2045.8	183.3	057	41.0	2317.5	174.1
R034	36.5	962.0	106.2	043A	37.5	1957.9	180.6	058	41.0	1620.4	124.3
035	37.5	1788.1	169.7	043B	36.5	1853.1	180.0	059	41.0	1545.7	120.2
R036	37.5	1047.6	108.2	049	36.5	794.2	91.0				
				NITROGEN							
005B	140	54.84	19.27	100	150	150.73	43.21	109	140	266.06	72.05
021RR	170	380.48	61.68	105	160	327.51	67.10	110	140	109.52	43.64
022RR	170	396.79	64.54	106A	165	356.31	65.45	111A	160	231.88	49.92
024RR	150	262.13	66.44	106B	165	356.00	66.67	111B	160	232.93	50.76
095	140	85.41	33.70	107	150	294.63	70.62	112	140	126.97	47.90
099	160	176.82	33.90	108	140	227.20	65.39				

Table 4.4 Calculated Data Used to Construct Nominal Isotherms for Liquid Hydrogen Inception

V_o (ft/sec)	h_o (ft, abs)	h_v (ft, abs)	K_{iv}	h_o (ft, abs)	h_v (ft, abs)	K_{iv}	h_o (ft, abs)	h_v (ft, abs)	K_{iv}
	Nominal Temp = 36.5°R			Nominal Temp = 37.5°R			Nominal Temp = 41.0°R		
70	581	481.77	1.30	643	569.25	0.97	952	981.82	--
80	681		2.00	747		1.79	1071		0.89
90	781		2.38	851		2.24	1189		1.65
100	885		2.59	959		2.51	1311		2.12
110	990		2.70	1068		2.65	1435		2.41
120	1099		2.76	1181		2.74	1562		2.59
130	1209		2.77	1296		2.77	1691		2.70
140	1324		2.77	1415		2.78	1825		2.77
150	1442		2.75	1537		2.77	1961		2.80
160	1564		2.72	1663		2.75	2101		2.82
170	1697		2.71	1800		2.74	2253		2.83
180	1849		2.72	1956		2.76	2423		2.86
185	1935	481.77	2.73	2044	569.25	2.77	2518	981.82	2.89

Table 4.5 Calculated Data Used to Construct Nominal Isotherms for Liquid Nitrogen Inception

V_o (ft/sec)	h_o (ft, abs)	h_v (ft, abs)	K_{iv} --
	Nominal Temp = 140°R		
20	56.0	44.40	1.87
25	63.5		1.97
30	73.5		2.08
35	85.0		2.13
40	99.0		2.20
45	116.0		2.28
50	136.5		2.37
55	161.5		2.49
60	190.0		2.60
65	221.5		2.70
70	254.0	44.40	2.75
	Nominal Temp = 165°R		
20	188.5	187.87	0.12
25	196.0		0.85
30	206.0		1.31
35	217.5		1.56
40	231.5		1.74
45	248.5		1.93
50	269.0		2.09
55	294.0		2.26
60	322.5		2.41
65	354.0		2.53
70	386.5	187.87	2.61

h_o (ft, abs)	h_v (ft, abs)	K_{iv} --
Nominal Temp = 150°R		
93.0	83.50	1.53
100.5		1.75
110.5		1.93
122.0		2.02
136.0		2.11
153.0		2.21
173.5		2.32
198.5		2.45
227.0		2.57
258.5		2.67
291.0	83.50	2.73
Nominal Temp = 170°R		
233.5	239.50	--
241.0		0.18
251.0		0.84
262.5		1.22
276.5		1.50
293.5		1.72
314.0		1.92
339.0		2.12
367.5		2.29
399.0		2.43
431.5	239.50	2.53

h_o (ft, abs)	h_v (ft, abs)	K_{iv} --
Nominal Temp = 160°R		
150.5	145.78	0.77
158.0		1.27
168.0		1.59
179.5		1.78
193.5		1.92
210.5		2.06
231.0		2.20
256.0		2.35
284.5		2.48
316.0		2.60
348.5	145.78	2.67

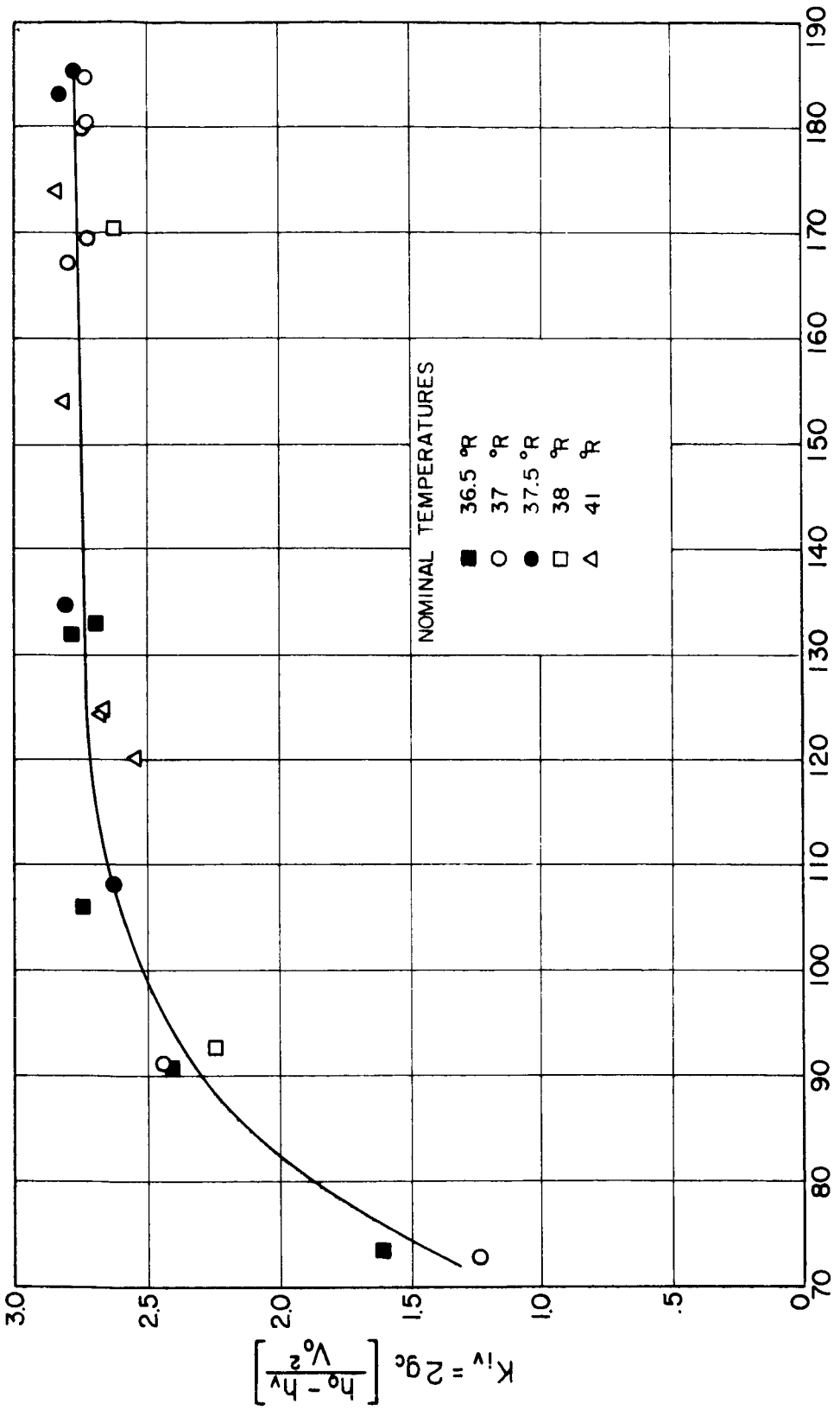

Figure 4.1 Cavitation Parameter for Liquid Hydrogen as Function of Test Section Inlet Velocity.

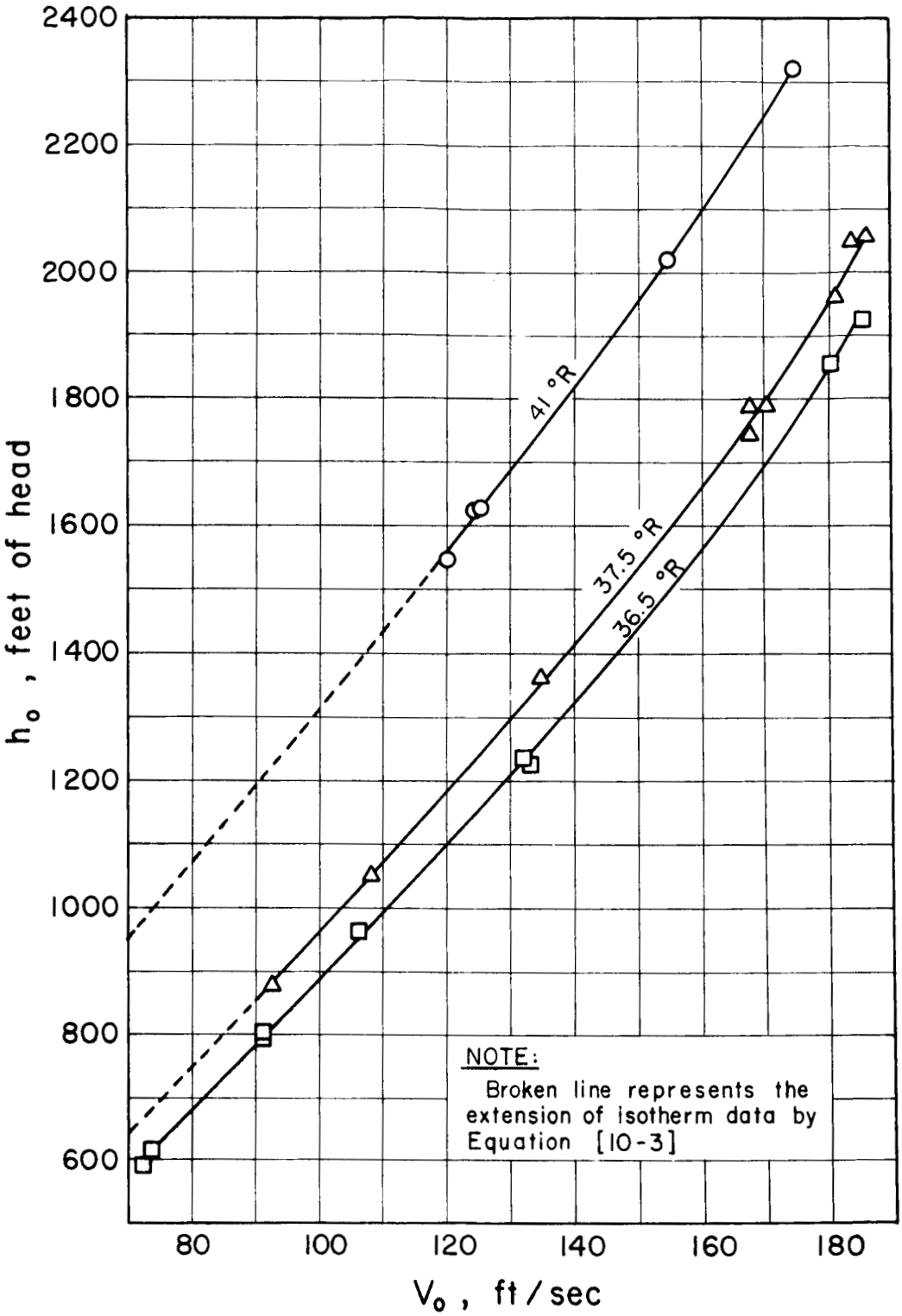

Figure 4.2 Effect of Test Section Inlet Velocity and Liquid Temperature on Required Inlet Head for Cavitation Inception in Liquid Hydrogen

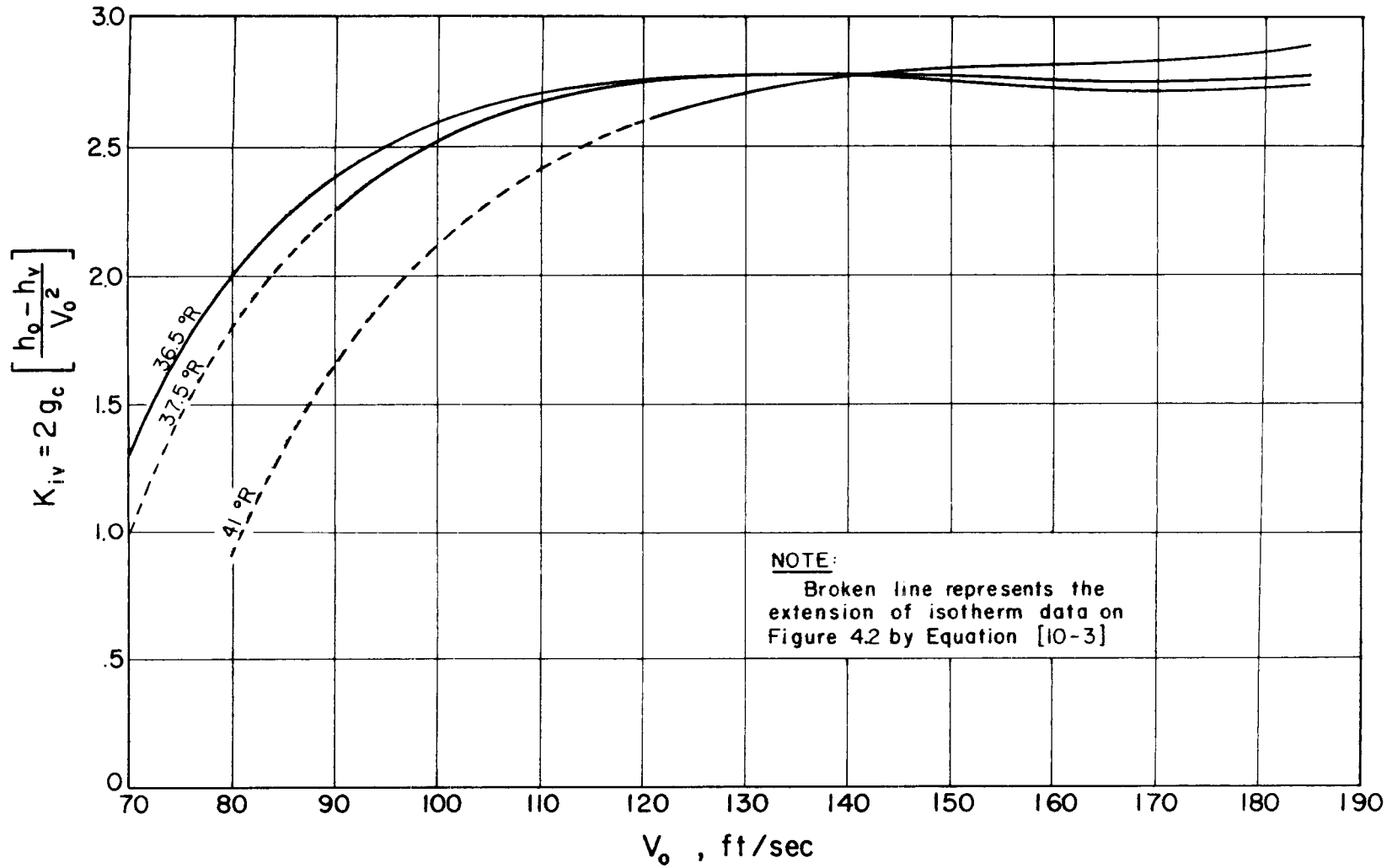

Figure 4.3 Cavitation Parameter for Liquid Hydrogen as a function of Test Section Inlet Velocity and Liquid Temperature.

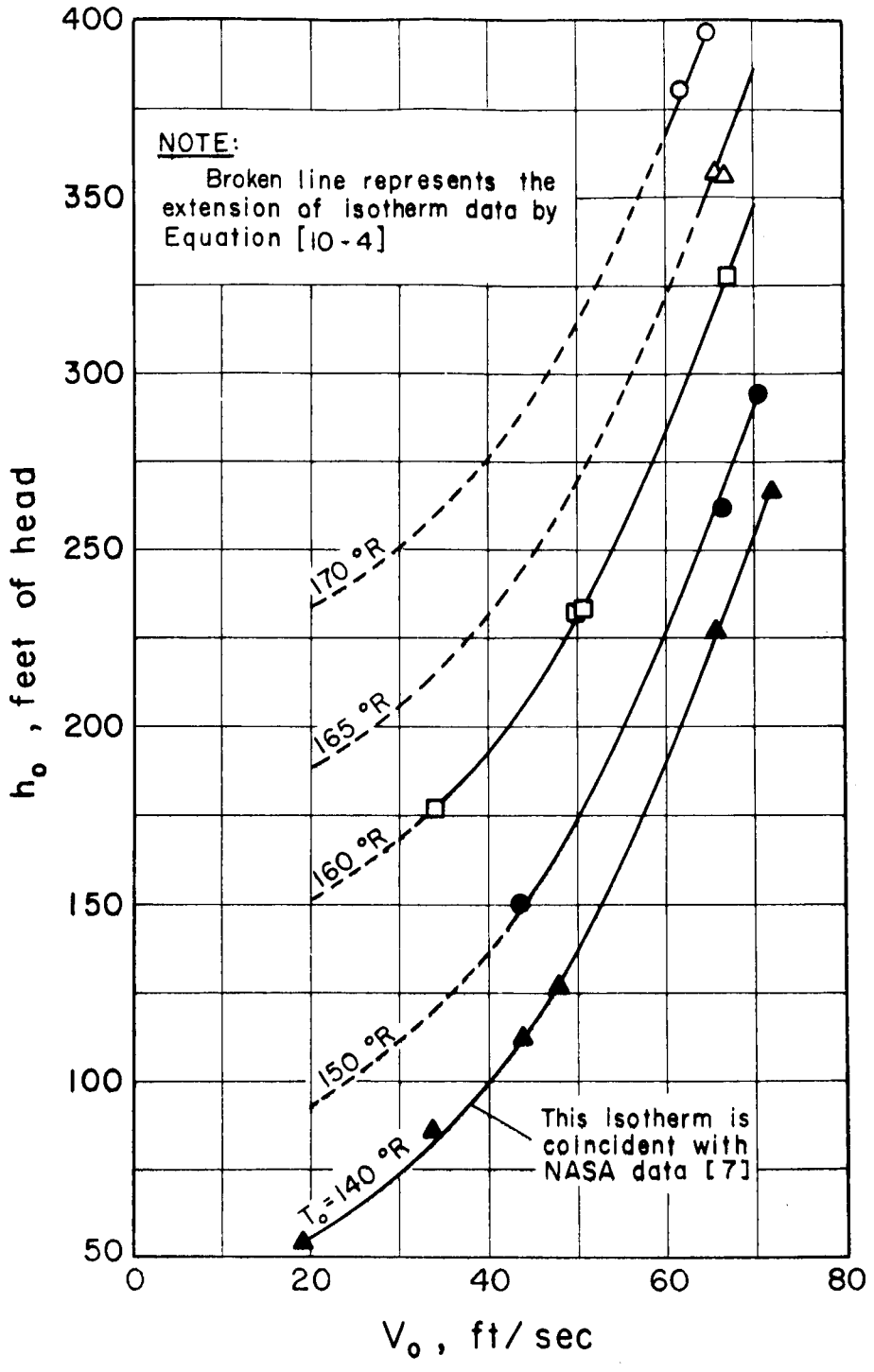

Figure 4.4 Effect of Test Section Inlet Velocity and Liquid Temperature on Required Inlet Head for Cavitation Inception in Liquid Nitrogen.

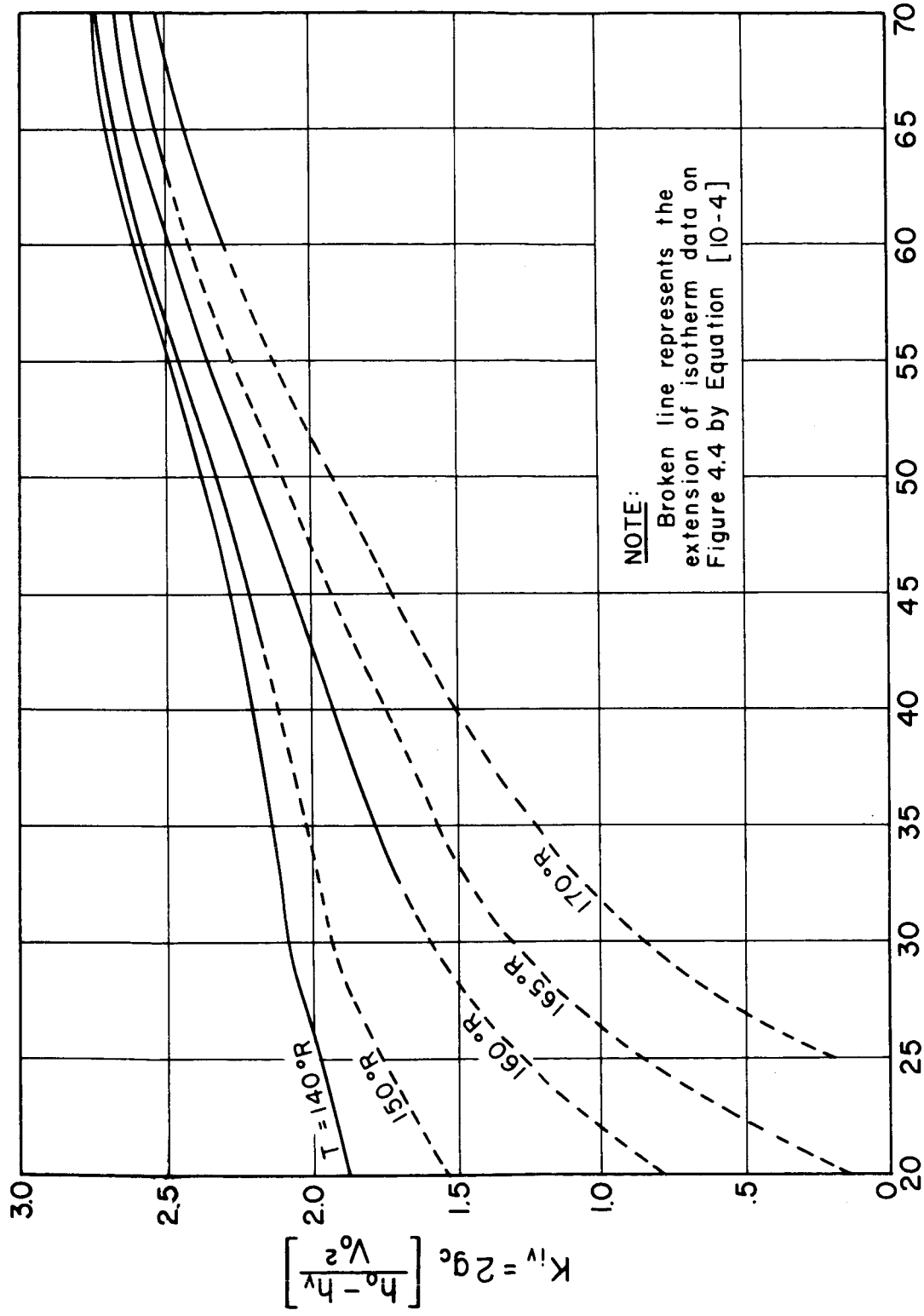

Figure 4.5 Cavitation Parameter for Liquid Nitrogen as Function of Test Section Inlet Velocity and Liquid Temperature.

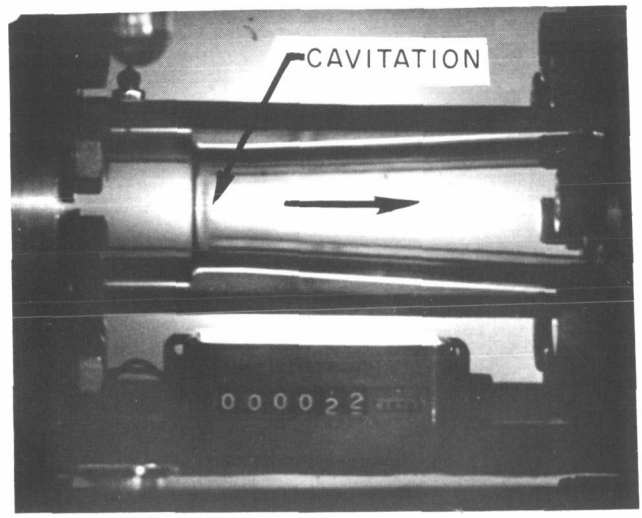

Figure 4.6 Photograph Showing Typical Cavitation Inception in Liquid Hydrogen

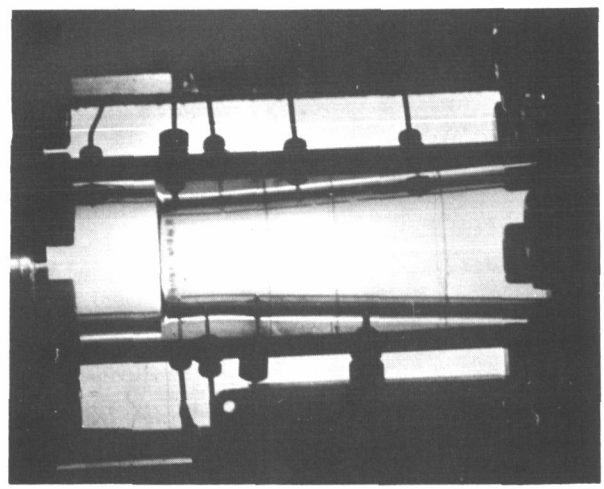

Figure 4.7 Photograph Showing Typical Cavitation Inception in Liquid Nitrogen

4.1 Data Analysis

Computed values of K_{iv} were plotted as a function of V_o for both hydrogen and nitrogen. However, inspection of the plots showed no readily discernable temperature dependence of K_{iv} for uncompensated experimental data (see figure 4.1; nitrogen is similar and is not shown).

The temperature dependence of K_{iv} is complicated by the fact that errors in the measured variable h_o are magnified in the calculation of K_{iv} as follows:

$$K_{iv} = 2g_c \left[\frac{h_o - h_v}{V_o^2} \right]; \qquad [4.1\text{-}1a]$$

differentiating [4.1-1a] at constant temperature and velocity there results,

$$dK_{iv} = \frac{2g_c}{V_o^2} dh_o. \qquad [4.1\text{-}1b]$$

The fractional change in K_{iv} due to a change dh_o is obtained by dividing [4.1-1b] by [4.1-1a],

$$\frac{dK_{iv}}{K_{iv}} = \frac{dh_o}{h_o - h_v}. \qquad [4.1\text{-}2]$$

The fractional change in h_o due to a change dh_o is by definition

$$\frac{dh_o}{h_o}.$$

The ratio of the fractional change in K_{iv} to the fractional change in h_o is obtained by dividing [4.1-2] by dh_o/h_o,

$$\frac{dK_{iv}/K_{iv}}{dh_o/h_o} = \frac{h_o}{h_o - h_v} \cdot \qquad [4.1\text{-}3]$$

Therefore any scatter which may occur in measuring h_o will be amplified by the term $\frac{h_o}{h_o - h_v}$, which has values as large as six for both hydrogen and nitrogen data given in this report.

Plots were also made of h_o as a function of V_o using the experimental data from this study. Both hydrogen and nitrogen data showed a distinct temperature dependence; however, there was sufficient experimental variation about each desired nominal liquid temperature to cause concern in constructing the individual isotherms. A nominal temperature or nominal isotherm is defined as that temperature which is selected to represent a specific group of data points with little temperature variation.

A technique was devised to evaluate the effect of temperature on the data and is detailed in Appendix B of this report.

4.2 Discussion of Data

It was pointed out earlier that no temperature dependence could be determined from K_{iv} vs V_o plots when the uncompensated experimental data were used, figure 4.1. However, once the nominal h_o vs V_o isotherms were established by mathematical temperature compensation, the K_{iv} vs V_o nominal isotherms may be computed from the basic definition of K_{iv}. Data on figures 4.2 and 4.4 represents the final "best-fit" of the experimental data points, "transferred" by means of equations [10-3] and [10-4] to the nominal isotherms shown. This method of presenting the h_o vs V_o data elminates the scatter due to experimental free-stream temperature variation. Good agreement was obtained with NASA data[7] for liquid nitrogen at 140°R; see figure 4.4. Since the NASA test section was 1.414 times as large as the plastic venturi described herein, negligible scale effects are indicated.

Minimum local wall pressure was calculated to be less than bulk stream vapor pressure by as much as 323 feet of hydrogen head and 63 feet of nitrogen head. These data are obtained by subtracting $\overset{v}{h}$ from h_v in tables 4.1 and 4.2.

Figures 4.3 and 4.5 are presented as a matter of interest, but it is to be noted that these K_{iv} curves depend entirely on the shape of the h_o vs V_o curves, and that errors in h_o are amplified in K_{iv} (as was shown earlier). Little variation in the shape of the h_o vs V_o curves is required to eliminate the inflection points in the corresponding K_{iv} vs V_o curves. The K_{iv} curves indicate the usual trends, i.e., K_{iv} increases with increasing velocities and decreasing temperatures. Figure 4.3 shows the isotherms for hydrogen intersecting at an inlet velocity of about 140 ft/sec. While this intersection is theoretically tenable, it could also be attributed to experimental data scatter. The data on figure 4.1 indicate little temperature dependence, and the data also suggests that K_{iv} may be invariant at inlet velocities greater than 140 ft/sec. Both hydrogen and nitrogen K_{iv} curves exhibit little temperature or velocity dependence at the higher velocities.

5. Summary

Cavitation inception parameters have been experimentally measured for liquid hydrogen and liquid nitrogen flowing in a clear plastic venturi. The experimental data points are given in table 4.1 for liquid hydrogen and table 4.2 for liquid nitrogen.

Temperature compensated values of inlet head, h_o versus inlet velocity, V_o, are presented on a background of mathematically temperature compensated isotherms; liquid hydrogen data are shown on figure 4.2 and liquid nitrogen data appear on figure 4.4. The 140°R isotherm constructed from the liquid nitrogen data is coincident with data furnished

by Ruggeri[7]. The venturi used in that experiment[4] was larger by a factor of 1.414:1; therefore, negligible scale effects are indicated. The mathematical technique used to temperature-compensate the experimental data is outlined in Appendix B of this paper.

Figure 4.1 shows experimental K_{iv} data points for liquid hydrogen; these data have not been temperature compensated and show no particular temperature trends. Temperature compensated values of the conventional cavitation parameter, K_{iv}, are also shown on figure 4.3 for liquid hydrogen and on figure 4.5 for liquid nitrogen: these curves have been derived from the smooth isotherms on the h_o vs V_o plots (figures 4.2 and 4.4). The data shows that K_{iv} increases with increasing velocities and decreases with increasing temperatures. At the higher velocities the K_{iv} curves indicate very little temperature or velocity dependence. The data used to construct figures 4.2 to 4.5 are given in tables 4.3 to 4.5.

The experiments showed that both liquid hydrogen and liquid nitrogen can sustain relatively large magnitudes of thermodynamic metastability; i.e., minimum local wall pressure was calculated to be considerably less than bulkstream vapor pressure. The magnitude of metastability for the various experiments is obtained by subtracting $\overset{v}{h}$ from h_v in tables 4.1 and 4.2.

6. Acknowledgements

A considerable number of people have been associated with this project at various times and their individual efforts are respectfully acknowledged. Mess'rs. Thomas T. Nagamoto, Dale R. Nielsen, Raymond V. Smith, and W. Harry Probert assisted in the early phases of apparatus assembly and experimentation. Mr. Peter Pemberton participated in some design modifications and Ajit Rapial was very helpful in the reduction and analysis of data. The photographic instrumentation and techniques used in this study are attributed to Thomas T. Theotokatos.

7. Nomenclature

A_o = test section inlet flow area [= 0.008063 ft^2]

C_p = pressure coefficient [$\equiv (h_x - h_o)/(V_o^2/2g_c)$]

$\overset{v}{C}_p$ = minimum pressure coefficient [$\equiv (\overset{v}{h} - h_o)/(V_o^2/2g_c)$]

$C_{n,(n=1,2---)}$ = constants appearing in equation [10-1] which are evaluated from best fit curves through h_o vs V_o data points

D_o = test section inlet diameter

g_c = conversion factor in Newton's law of motion, given in engineering units as g_c = 32.2(ft)(pounds mass)/(sec^2) (pounds force)

h_o = test section inlet head corresponding to absolute inlet pressure, ft

$h_{o,1}$ = value of inlet head corresponding to a data point before it is "transferred" to a new position, ft

$h_{o,2}$ = value of inlet head corresponding to a data point after it has been "transferred" to a new position, ft

h_v = head corresponding to saturation or vapor pressure at test section inlet temperature, ft

h_x = head corresponding to absolute pressure measured at wall of plastic venturi at distance x downstream of the minimum pressure point, ft

$\check{h}$ = head corresponding to minimum absolute pressure on quarter round of plastic venturi contour, ft, computed from expression for $\check{C}_p$

K_{iv} = incipient cavitation parameter $[\equiv(h_o - h_v)/(V_o^2/2g_c)]$

$\dot{m}$ = mass flow rate, e.g., (pounds mass)/sec

P_o = test section absolute inlet pressure

P_v = saturation or vapor pressure at test section inlet temperature

$(Re)_{D_o}$ = Reynolds number based on test section inlet diameter

T_o = temperature in degrees Rankine, of bulk fluid entering the test section

$T_{o,1}$ = the inlet temperature from which a data point is to be "transferred"

$T_{o,2}$ = the inlet temperature to which a data point is being "transferred"

$T_{o,B}$ = the nominal temperature chosen for construction of a "base" isotherm due to the availability of sufficient h_o vs V_o data at or near that temperature

T_o' = a nominal isotherm on a h_o vs V_o plot

T_o'' = a nominal isotherm, different from T_o', on a h_o vs V_o plot

V_o = velocity of test fluid at inlet to venturi test section

x = distance measured from minimum pressure point on quarter-round contour along axis of plastic venturi

8. References

1. Pinkel, I. I., M. J. Hartmann, C. H. Hauser, M. J. Miller, R. S. Ruggeri, and R. F. Soltis, Pump Technology, Chap. VI, pp. 81-101, taken from Conference on Selected Technology for the Petroleum Industry, NASA SP-5053 (1966).

2. Erosion by Cavitation or Impingement, STP 408, 288 pages (1967), Available from ASTM, 1916 Race Street, Phila., Pa., 19103.

3. Ruggeri, R. S. and T. F. Gelder, Effects of Air Content and Water Purity on Liquid Tension at Incipient Cavitation in Venturi Flow, NASA TN D-1459, (1963).

4. Ruggeri, R. S. and T. F. Gelder, Cavitation and Effective Liquid Tension of Nitrogen in a Tunnel Venturi, NASA TD-2088, (1964).

5. Gelder, T. F., R. D. Moore, and R. S. Ruggeri, Incipient Cavitation of Freon-114 in a Tunnel Venturi, NASA TN D-2662, (1965).

6. Ruggeri, R. S., R. D. Moore, and T. F. Gelder, Incipient Cavitation of Ethylene Glycol in a Tunnel Venturi, NASA TN D-2772, (1965).

7. Ruggeri, R. S., Private communication.

8. Flow Measurement, Chap. 4, Part 5 - Measurement of quantity of materials, p. 17, PTC-19.5;4-1959, the American Society of Mechanical Engineers, 29 West 39th St., New York 18, N. Y.

9. Kittredge, C. P., Detection and Location of Cavitation, Plasma Physics Lab, Princeton Univ., Princeton, N. J., Report MATT-142 (Aug. 1962). Available from O. T. S., U. S. Dept. of Commerce, Washington 25, D. C.

10. Lehman, A. F. and J. O. Young, Experimental Investigations of Incipient and Desinent Cavitation, ASME Paper No. 63-AHGT-20 (Mar. 1963).

11. Holl, J. W., Discussions of Symposium on Cavitation Research Facilities and Techniques, Presented at Fluids Engr'g. Div. Confer. Phila., Pa., May 18-20, 1964, Available from ASME, United Engineering Center, 345 East 47th St., New York 17, N. Y.

9. Appendix A---Acoustic Detector

A detailed drawing of the acoustic transducer is given on figure 9.1 and a schematic of the instrument hook-up is given on figure 9.2.

The transducer consists of a Barium-Titanate piezoelectric crystal sandwiched between the body of the transducer and a machine screw, figure 9.1. The mechanical coupling or initial compression level in the crystal could be varied by means of the machine screw. Thus, the sensitivity of the crystal to mechanical vibration could be adjusted somewhat. Electrical leads were attached to the adjustment screw and to the body of the transducer. Coaxial electrical wire was used to connect the transducer to a cathode-follower-amplifier, see figure 9.2. The signal was then filtered through a variable band-pass filter and displayed on an oscilloscope. The band-pass filter was set to admit signal frequencies of 3 to 200 k-Hz for most tests.

The acoustic transducer was screw-mounted in the downstream flange of the plastic venturi via pipe threads. Most of the system vibration and noise appeared to be of low frequency and was easily eliminated with the band-pass filter.

Cavitation was readily discernable on the oscilloscope and was characterized by large-amplitude, high-frequency signals.

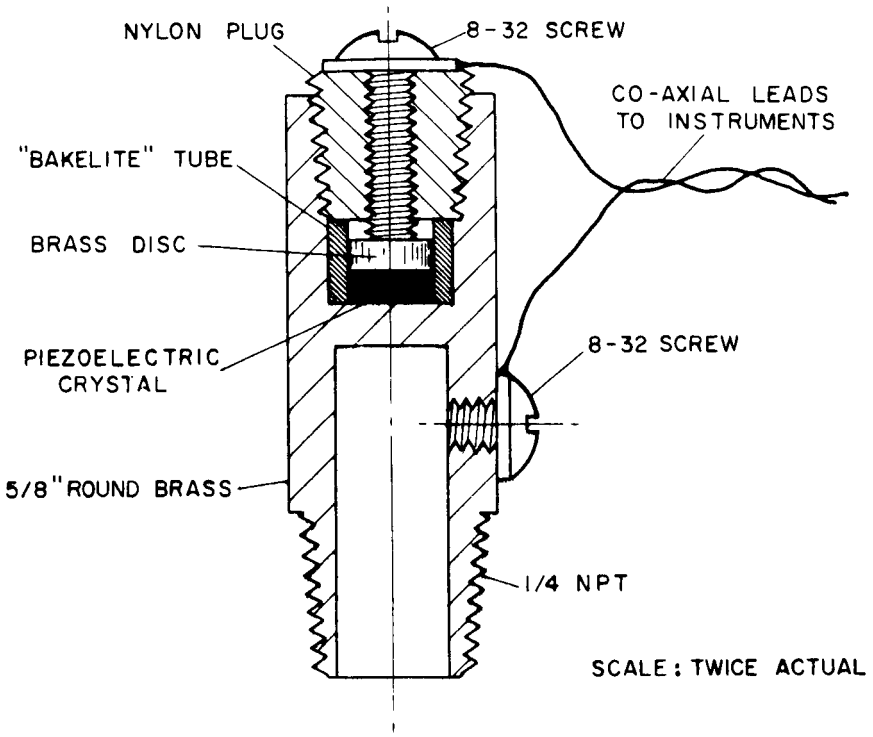

Figure 9.1 Acoustic Transducer for Detection of Cavitation Inception.

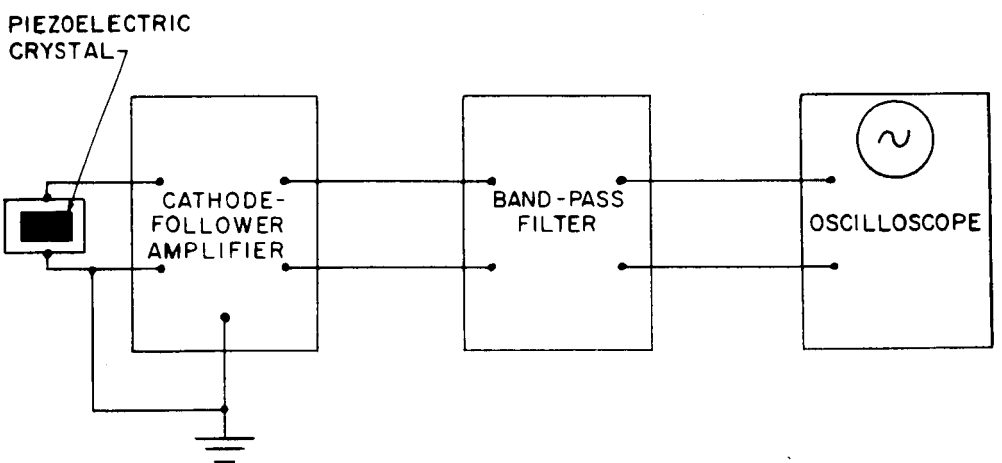

Figure 9.2 Block Diagram of Signal Conditioning Instruments Used with Acoustic Cavitation Detection Device.

10. Appendix B---Method Used to Compensate the Experimental Inception Data for Temperature Deviation about the Nominal Isotherms

(1) It was assumed that a change in inlet temperature, dT_o, will produce a change in inlet head, dh_o, along a constant velocity path, which will be a function of the velocity and temperature only; it is also assumed that this function may be approximated by a few terms of a polynomial. Justification of these assumptions is evidenced by the good results which were obtained for both hydrogen and nitrogen (see figures 4.2 and 4.4) by using the following equation:

$$dh_o = [C_1 T_o^2 + C_2 T_o + C_3 V_o^2 + C_4 V_o + C_5]\, dT_o. \qquad [10\text{-}1]$$

Holding V_o constant and integrating from $h_{o,1}$ to $h_{o,2}$ and from $T_{o,1}$ to $T_{o,2}$ there results:

$$\left[h_{o,2} - h_{o,1}\right]_{V_o} = C_1'[(T_{o,2})^3 - (T_{o,1})^3] + C_2'[(T_{o,2})^2 - (T_{o,1})^2] + (T_{o,2} - T_{o,1})(C_3 V_o^2 + C_4 V_o + C_5), \qquad [10\text{-}2]$$

where the subscript "1" refers to the position of a data point before it is transferred to a new position identified by the subscript "2".

For each of the following steps (two through seven) there is a corresponding graphical illustration on Figure 10.1.

(2) h_o vs V_o experimental data were plotted, a separate graph being used for each test fluid. The data points were identified with their individual temperatures so that "best-fit" curves could be drawn through each group of data points having a common nominal temperature. A nominal temperature is defined as that temperature which is selected to

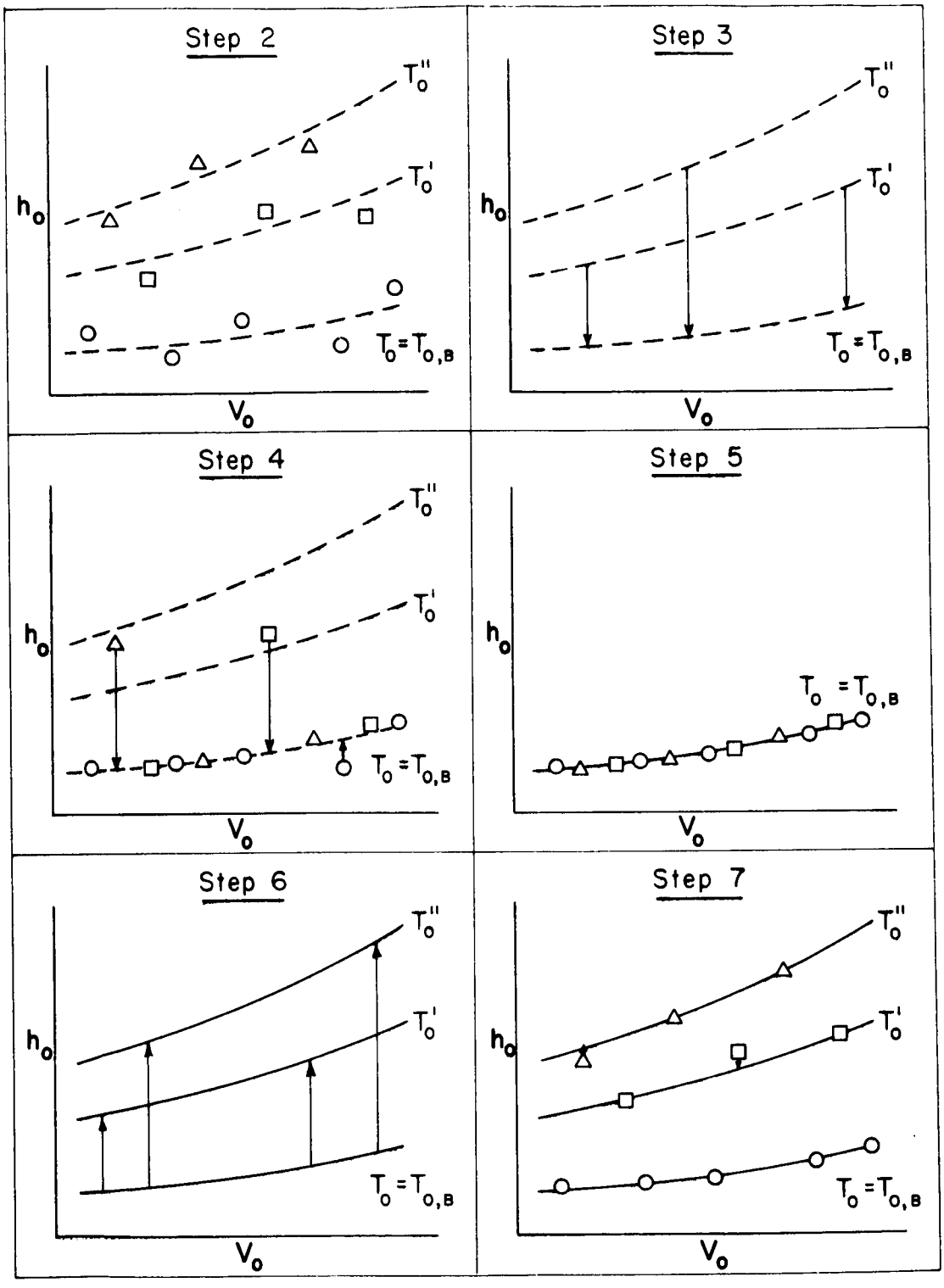

Figure 10.1 Illustration of Method Used to Construct Nominal Isotherms from Experimental Data

represent a specific group of data points having little temperature variation. These first-approximation isotherms are shown as dashed lines on step two of figure 10.1.

One of the nominal isotherms is chosen, on the basis of availability of sufficient experimental h_o vs V_o data at or near that temperature, as a reference or "base" isotherm for succeeding computations. This isotherm is designated $T_{o,B}$ in figure 10.1 while the other isotherms are designated T_o' and T_o''.

(3) The constants in equation [10-2] are evaluated by selecting pairs of values of h_o and T_o from the nominal isotherms at identical velocities as follows: on figure 10.1 the tail of each arrow indicates a value of $h_{o,1}$ and $T_{o,1}$ while the arrow head points to $h_{o,2}$ and $T_{o,2}$. The coordinate points from each arrow are then used in equation [10-2]. Note that each arrow provides one equation, hence five arrows are needed to evaluate the constants in [10-2]. The arrows always follow a constant velocity path and must be strategically placed in order for the five equations to be independent. The actual data points are not shown since they are not used in this step. The equation derived from this step will "transfer" data from one temperature to another within the confines of the bounding isotherms.

(4) In step four of the illustration, arrows are used to indicate the "transferral" of experimental data points to a new location near the base isotherm. $h_{o,1}$ and $T_{o,1}$ are known from the experimental data, while $T_{o,2}$ is simply the base nominal temperature, $T_{o,B}$; values of $h_{o,2}$ can then be determined, by using equation [10-2], and plotted near the base temperature, $T_{o,B}$. Note that the data transfer always follows a constant velocity path.

(5) A new "best fit" isotherm can then be drawn through all of the "transferred" data points at $T_{o,B}$. This new curve is shown as a solid line in figure 10.1; the first approximation isotherms, drawn as dashed lines, are no longer needed and are omitted in the illustration of this step. The curve obtained from this step represents an improved reference isotherm.

(6) The new reference isotherm and equation [10-2] may now be used to reconstruct the other nominal isotherms. T_o' and T_o'' may be reconstructed by using equation [10-2] and $h_{o,1}$ values from the new base isotherm. Note that $T_{o,B}$ now becomes $T_{o,1}$ and T_o' and T_o'' take their respective turns as $T_{o,2}$. Values of $h_{o,2}$ are then computed in order to plot the two new isotherms shown in the illustration of this step on figure 10.1.

(7) The original experimental data points were then transferred to their nearest nominal temperature by means of equation [10-2]. Those points having a nominal temperature of $T_{o,B}$ were relocated in their final position in step four. This process brings the data points near their respective isotherms, as shown by the arrows in the illustration of step seven. Note that $h_{o,2}$ is again the only unknown in equation [10-2].

(8) The agreement between the new nominal isotherms and the transferred experimental data points was then observed: If the fit was not satisfactory, "best-fit" curves were drawn through the "transferred" data points and the entire computational procedure---steps (3) through (7)--- was repeated. Several iterations were necessary to obtain suitable mathematical expressions for liquid hydrogen and liquid nitrogen: tables 4.3, 4.4, and 4.5 as well as figures 4.2 and 4.4 were prepared by using the following equations.

Hydrogen:

$$\left[h_{o,2} - h_{o,1}\right]_{V_o} \approx 5.86\left[(T_{o,2})^2 - (T_{o,1})^2\right]$$

$$+(T_{o,2} - T_{o,1})(0.41\, V_o - 400.35). \qquad [10\text{-}3]$$

Nitrogen:

$$\left[h_{o,2} - h_{o,1}\right]_{V_o} \approx 0.000835\left[(T_{o,2})^3 - (T_{o,1})^3\right]$$

$$-0.2729\left[(T_{o,2})^2 - (T_{o,1})^2\right] + 30.152\,(T_{o,2} - T_{o,1}). \qquad [10\text{-}4]$$

It should be noted that some of the terms in equation [10-2] become negligible and consequently are not included in [10-3] and [10-4]. It is observed that equation [10-3] for hydrogen is velocity dependent, while equation [10-4] for nitrogen is not. It is not recommended that equations [10-3] and [10-4] be used outside the general area of the data points given.

11. Appendix C

DISTRIBUTION LIST FOR INTERIM REPORT NASA CR-72285

Contract C-35560A

		Copies
National Aeronautics and Space Administration Lewis Research Center 21000 Brookpark Road Cleveland, Ohio 44135		
Attention:	Contracting Officer, MS 500-313	1
	Liquid Rocket Technology Branch, MS 500-209	8
	Technical Report Control Office, MS 5-5	1
	Technology Utilization Office, MS 3-16	1
	AFSC Liaison Office, MS 4-1	2
	Library, MS 60-3	2
	D. L. Nored, MS 500-209	1
	W. E. Roberts, MS 3-17	1
	E. W. Conrad, MS 100-1	1
	Fluid Systems Components Division, MS 5-3	1
National Aeronautics and Space Administration Washington, D. C. 20546		
Attention:	Code MT	1
	RPX	2
	RPL	2
	SV	1
	Jack Suddreth, RPL	1
Scientific and Technical Information Facility P. O. Box 33 College Park, Maryland 20740		
Attention:	NASA Representative Code CRT	6
National Aeronautics and Space Administration Ames Research Center Moffett Field, California 94035		
Attention:	Library	1
	C. A. Syvertson	1

	Copies
National Aeronautics and Space Administration Flight Research Center P. O. Box 273 Edwards, California 93523	
Attention: Library	1
National Aeronautics and Space Administration Goddard Space Flight Center Greenbelt, Maryland 20771	
Attention: Library	1
National Aeronautics and Space Administration John F. Kennedy Space Center Cocoa Beach, Florida 32931	
Attention: Library	1
National Aeronautics and Space Administration Langley Research Center Langley Station Hampton, Virginia 23365	
Attention: Library	1
National Aeronautics and Space Administration Manned Spacecraft Center Houston, Texas 77001	
Attention: Library	1
National Aeronautics and Space Administration George C. Marshall Space Flight Center Huntsville, Alabama 35812	
Attention: Library	1
Keith Chandler, R-P&VE-PA	1
Loren Gross, R-P&VE-PAC	1
J. L. Vaniman, R-P&VE-PTP	1
Hugh Campbell, R-P&VE-PEC	1
National Aeronautics and Space Administration Western Operations Office 150 Pico Boulevard Santa Monica, California 90406	
Attention: Library	1

	Copies
Jet Propulsion Laboratory 4800 Oak Grove Drive Pasadena, California 91103	
Attention: Library	1
Henry Burlage	1
Office of the Director of Defense Research & Engineering Washington, D. C. 20301	
Attention: Dr. H. W. Schulz, Office of Asst. Dir. (Chem. Technology)	1
Defense Documentation Center Cameron Station Alexandria, Virginia 22314	1
RTD(RTNP) Bolling Air Force Base Washington, D. C. 20332	1
Arnold Engineering Development Center Air Force Systems Command Tullahoma, Tennessee 37390	
Attention: AEOIM	1
Advanced Research Projects Agency Washington, D. C. 20525	
Attention: D. E. Mock	1
Aeronautical Systems Division Air Force Systems Command Wright-Patterson Air Force Base, Dayton, Ohio 45433	
Attention: D. L. Schmidt, Code ASRCNC-2	1
Air Force Missile Test Center Patrick Air Force Base, Florida 32925	
Attention: L. J. Ullian	1

	Copies
Air Force Systems Command (SCLT/Capt. S. W. Bowen) Andrews Air Force Base Washington, D. C. 20332	1
Air Force Rocket Propulsion Laboratory (RPR) Edwards, California 93523	1
Air Force Rocket Propulsion Laboratory (RPM) Edwards, California 93523	1
Air Force FTC (FTAT-2) Edwards Air Force Base, California 93523	
Attention: Col. J. M. Silk	1
Air Force Office of Scientific Research Washington, D. C. 20333	
Attention: SREP, Dr. J. F. Masi	1
Office of Research Analyses (OAR) Holloman Air Force Base, New Mexico 88330	
Attention: RRRT	1
Maj. R. E. Brocken, Code MDGRT	1
U. S. Air Force Washington, D. C. 20330	
Attention: Col. C. K. Stambaugh, Code AFRST	1
Commanding Officer U. S. Army Research Office (Durham) Box CM, Duke Station Durham, North Carolina 27706	1
U. S. Army Missile Command Redstone Scientific Information Center Redstone Arsenal, Alabama 35808	
Attention: Chief, Document Section	1
Dr. W. Wharton	1

	Copies
Bureau of Naval Weapons Department of the Navy Washington, D. C. 20360	
Attention: J. Kay, Code RTMS-41	1
Commander U. S. Naval Ordnance Test Station China Lake, California 93557	
Attention: Code 45	1
Code 753 (Library)	1
Commanding Officer Office of Naval Research 1030 E. Green Street Pasadena, California 91101	1
Director (Code 6180) U. S. Naval Research Laboratory Washington, D. C. 20390	
Attention: H. W. Carhart	1
Picatinny Arsenal Dover, New Jersey	
Attention: I. Forsten, Chief Liquid Propulsion Laboratory	1
U. S. Atomic Energy Commission Technical Information Services Box 62 Oak Ridge, Tennessee 37831	
Attention: A. P. Huber, Code ORGDP Box P	1
Air Force Aero Propulsion Laboratory Research & Technology Division Air Force Systems Command United States Air Force Wright-Patterson AFB, Ohio 45433	
Attention: APRP (C. M. Donaldson)	1

	Copies
Aerojet-General Corporation P. O. Box 296 Azusa, California 91703	
Attention: Librarian	1
Aerojet-General Corporation 11711 South Woodruff Avenue Downey, California 90241	
Attention: F. M. West, Chief Librarian	1
Aerojet-General Corporation P. O. Box 1947 Sacramento, California 95809	
Attention: Technical Library 2484-2015A	1
Aeronutronic Division of Philco Corporation Ford Road Newport Beach, California 92600	
Attention: Dr. L. H. Linder, Manager	1
Technical Information Department	1
Aerospace Corporation P. O. Box 95085 Los Angeles, California 90045	
Attention: Library-Documents	1
Arthur D. Little, Incorporated Acorn Park Cambridge, Massachusetts 02140	
Attention: A. C. Tobey	1
ARO, Incorporated Arnold Engineering Development Center Arnold AF Station, Tennessee 37389	
Attention: Dr. B. H. Goethert Chief Scientist	1

	Copies
Atlantic Research Corporation Shirley Highway & Edsall Road Alexandria, Virginia 22314	
Attention: Security Office for Library	1
Battelle Memorial Institute 505 King Avenue Columbus, Ohio 43201	
Attention: Report Library, Room 6A	1
Beech Aircraft Corporation Boulder Facility Box 631 Boulder, Colorado 80302	
Attention: Library	1
Bell Aerosystems, Incorporated Box 1 Buffalo, New York 14205	
Attention: Library	1
Bendix Systems Division Bendix Corporation Ann Arbor, Michigan 48106	
Attention: Library	1
The Boeing Company Aero Space Division P. O. Box 3707 Seattle, Washington 98124	
Attention: Ruth E. Peerenboom (1190)	1
Chemical Propulsion Information Agency Applied Physics Laboratory 8621 Georgia Avenue Silver Spring, Maryland 20910	1
Chrysler Corporation Space Division New Orleans, Louisiana 70150	
Attention: Librarian	1

	Copies
Curtiss-Wright Corporation Wright Aeronautical Division Wood-Ridge, New Jersey 07075	
Attention: G. Kelley	1
University of Denver Denver Research Institute P. O. Box 10127 Denver, Colorado 80210	
Attention: Security Office	1
Douglas Aircraft Company, Inc. Santa Monica Division 3000 Ocean Park Boulevard Santa Monica, California 90405	
Attention: Library	1
Fairchild Stratos Corporation Aircraft Missiles Division Hagerstown, Maryland 20740	
Attention: J. S. Kerr	1
General Dynamics/Astronautics P. O. Box 1128 San Diego, California 92112	
Attention: Library & Information Services (128-00)	1
Convair Division General Dynamics Corporation P. O. Box 1128 San Diego, California 92112	
Attention: Mr. W. Fenning Centaur Resident Project Office	1
General Electric Company Flight Propulsion Lab. Department Cincinnati, Ohio 45215	
Attention: D. Suichu	1

	Copies
Grumman Aircraft Engineering Corporation Bethpage, Long Island, New York 11714	
Attention: Joseph Gavin	1
ITT Research Institute Technology Center Chicago, Illinois 60616	
Attention: Library	1
Kidde Aero-Space Division Walter Kidde & Company, Inc. 675 Main Street Belleville, New Jersey 07109	
Attention: R. J. Hanville, Director of Research Engineering	1
Lockheed Missiles & Space Company P. O. Box 504 Sunnyvale, California 94088	
Attention: Technical Information Center	1
Lockheed Propulsion Company P. O. Box 111 Redlands, California 92374	
Attention: Miss Belle Berlad, Librarian	1
Lockheed Missiles & Space Company Propulsion Engineering Division (D. 55-11) 1111 Lockheed Way Sunnyvale, California 94087	1
Marquardt Corporation 16555 Saticoy Street Box 2013 - South Annex Van Nuys, California 91404	
Attention: Librarian	1
Purdue University Lafayette, Indiana 47907	
Attention: Technical Librarian	1

	Copies
Rocketdyne, A Division of North American Rockwell Corporation 6633 Canoga Avenue Canoga Park, California 91304	
Attention: Library, Department 596-306	1
Stanford Research Institute 333 Ravenswood Avenue Menlo Park, California 94025	
Attention: Thor Smith	1
TRW Systems, Incorporated One Space Park Redondo Beach, California 90200	
Attention: G. W. Elverum	1
STL Tech. Lib. Doc. Acquisitions	1
TRW, Incorporated TAPCO Division 23555 Euclid Avenue Cleveland, Ohio 44117	
Attention: P. T. Angell	1
United Aircraft Corporation Corporation Library 400 Main Street East Hartford, Connecticut 06118	
Attention: Library	1
Frank Owen	1
W. E. Taylor	1
United Aircraft Corporation Pratt and Whitney Division Florida Research and Development Center P. O. Box 2691 West Palm Beach, Florida 33402	
Attention: Library	1

	Copies
California Institute of Technology Pasadena, California 91109	
Attention: Dr. A. Acosta	1
Dr. A. T. Ellis	1
Prof. M. S. Plesset	1
The Pennsylvania State University Ordnance Research Laboratory P. O. Box 30 State College, Pennsylvania 16801	
Attention: Prof. G. F. Wislicenus	1
Dr. J. W. Holl	1
Hydronautics, Incorporated Pendell School Road Howard County Laurel, Maryland 20810	
Attention: Dr. Philip Eisenberg	1
St. Anthony Falls Hydraulic Laboratory Mississippi River at Third Avenue, S.E. Minneapolis, Minnesota 55414	
Attention: Prof. J. F. Ripkin	1
State University of New York-Buffalo Mechanical Engineering Department Buffalo, New York 14214	
Attention: Dr. Virgil J. Lunardini	1
Commander U. S. Naval Missile Center Point Mugu, California 93041	
Attention: Technical Library	1